

Galaxy-wide outflows: cold gas and star formation at high speeds

Kastytis Zubovas¹ and Andrew R. King²

¹ *Center for Physical Sciences and Technology, Savanorių 231, Vilnius LT-02300, Lithuania*

² *Theoretical Astrophysics Group, University of Leicester, Leicester LE1 7RH, U.K.*

E-mail: kastytis.zubovas@ftmc.lt

3 January 2014

ABSTRACT

Several active galaxies show strong evidence for fast ($v_{\text{out}} \sim 1000 \text{ km s}^{-1}$) massive ($\dot{M} = \text{several} \times 1000 \text{ M}_{\odot} \text{ yr}^{-1}$) gas outflows. Such outflows are expected on theoretical grounds once the central supermassive black hole reaches the mass set by the $M - \sigma$ relation, and may be what makes galaxies become red and dead. Despite their high velocities, which imply temperatures far above those necessary for molecule dissociation, the outflows contain large amounts of molecular gas. To understand this surprising result, we investigate the gas cooling and show that the outflows cannot stably persist in high-temperature states. Instead the outflowing gas forms a two-phase medium, with cold dense molecular clumps mixed with hot tenuous gas, as observed. We also show that efficient cooling leads to star formation, providing an observable outflow signature. The central parts of the outflows can be intrinsically luminous gamma-ray sources, provided that the central black hole is still strongly accreting. We note also that these outflows can persist for $\sim 10^8 \text{ yr}$ after the central AGN has turned off, so that many observed outflows (particularly with high speeds) otherwise assumed to be driven by starbursts might also be of this type.

Key words: galaxies: evolution — quasars: general — black hole physics — accretion, accretion disks

1 INTRODUCTION

Over the past decade, observations revealed mounting evidence of strong outflows from active galactic nuclei (AGN), which significantly affect the evolution of their host galaxies. Highly ionized relativistic winds (e.g. Pounds et al. 2003b,a; Pounds & Vaughan 2011) and kiloparsec-scale outflows (Feruglio et al. 2010; Sturm et al. 2011; Rupke & Veilleux 2011) have been detected in active galaxies, with total kinetic luminosities L_{kin} equal to a few percent of the AGN luminosity.

The basic properties of large scale outflows – mass and momentum flow rate, velocity $v_{\text{out}} \sim 1000 \text{ km/s}$, kinetic energy – can be well explained by the model of AGN wind feedback, first proposed by King (2003) and later developed both analytically (King 2005, 2010b; Zubovas & King 2012a; Faucher-Giguère & Quataert 2012) and numerically (Nayakshin & Power 2010; Zubovas & Nayakshin 2012). Within this model, AGN radiation pressure launches a relativistic wind from very close in, where the Thomson scattering optical depth self-regulates to be $\tau = 1$. The wind then shocks against the surrounding gas and drives an outflow. If the mass of the supermassive black hole (SMBH) that

powers the AGN exceeds the critical mass given by

$$M_{\sigma} \simeq \frac{f_c \kappa \sigma^4}{\pi G^2} \simeq 3.67 \times 10^8 \sigma_{200}^4 \text{ M}_{\odot}, \quad (1)$$

where $f_c = 0.16$ is the cosmological ratio of gas density to matter density, $\kappa \simeq 0.4 \text{ cm}^2/\text{g}$ is the electron scattering opacity and $\sigma \equiv 200 \sigma_{200} \text{ km/s}$ is the velocity dispersion in the host galaxy spheroid, its wind shocks can propagate out to large distances and are no longer efficiently Compton cooled. As a result, the previously weak and cold, momentum-driven outflows change character to become energy-driven. These outflows are far more violent, and clear galaxies of gas (Zubovas & King 2012a), leaving them red and dead.

The observed large-scale outflows contain mostly molecular gas. This is, in principle, a problem for the AGN wind feedback model, because outflowing gas is accelerated by a shock and heated to temperatures of $10^6 - 10^7 \text{ K}$, much higher than molecular dissociation temperatures. Although cold clumps could be embedded in the ambient medium and carried with the flow, such acceleration would produce signatures incompatible with observations (Cicone et al. 2012).

We show here that radiative cooling rapidly puts a

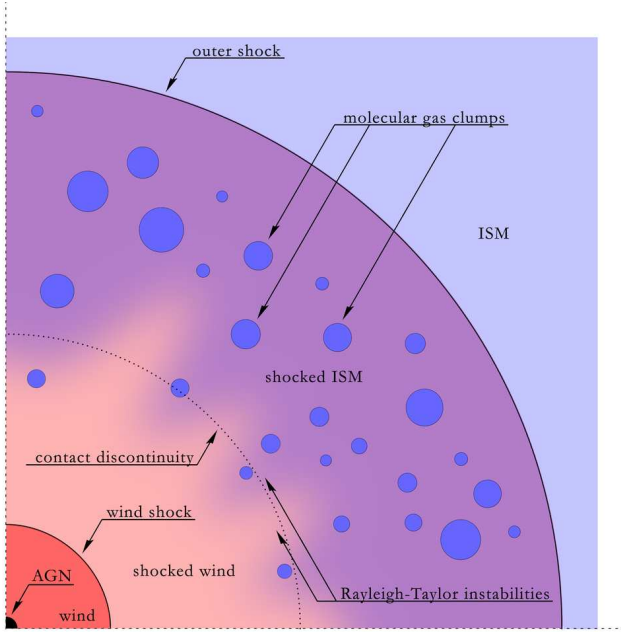


Figure 1. A schematic view of the multiphase nature of the energy-driven outflow launched when the central supermassive black hole reaches the critical $M - \sigma$ mass. The AGN drives a powerful quasi-spherical wind with speed $v \sim 0.1c$ from its accretion disc. This wind is strongly shocked just outside the inner Compton cooling radius (radius $R_{IC} \sim 0.5M_8/\sigma_{200}$ kpc, where M_8 is the black hole mass in units of $10^8 M_\odot$). The expanding shocked wind sweeps up and drives an outer shock into the host ISM. The contact discontinuity between the expanding wind gas and swept-up ISM is Rayleigh–Taylor unstable, so these two components mix together in the outflow and help maintain a constant pressure. The outflow cools radiatively, and most of it freezes out into clumps of cold molecular material. Despite its high velocity $v \sim 1000 \text{ km s}^{-1}$ most of the outflow is in molecular form. The very high temperature of the wind shock near R_{IC} implies that these outflows should be intrinsically luminous gamma-ray sources.

large fraction of the outflowing material into molecular form, which stably coexists with tenuous hot gas. This simultaneously explains the large velocity of the molecular component and its immunity to high Mach number shocks, in agreement with observations (Cicone et al. 2012). We review the properties of the forward shock that the outflow drives into the ISM in Section 2 and show that it cannot be kept thermally stable at high temperatures by quasar radiation in Section 3. We then consider the cooling of its gas in Section 4 and estimate the rate of star formation in the cooling outflow in Section 5. Finally, we discuss our results in Section 6 and summarize giving predictions for observations in Section 7.

2 THE OUTER SHOCK

The dynamics of spherically-symmetric energy-driven outflows from accreting AGN are described in King (2005) and Zubovas & King (2012a). We briefly summarize this subject here, to establish the properties of the outflow relevant for the present problem.

Rapidly accreting AGN launch fast ($v_w \sim 0.1c$) winds

from their accretion discs. The wind shocks against the surrounding ISM and drives an outflow. Close to the black hole, the shocked wind cools rapidly by the inverse Compton effect of the AGN radiation field, and the resulting outflow of swept-up gas is relatively slow and must ultimately fall back. But once the mass of the central black hole grows above the critical value M_σ (eq. 1), the wind shock and swept-up ISM can reach large radii, where the AGN radiation field is too dilute to cool the shocked wind gas. Now all of the wind energy goes into powering the outflow, rather than almost all being lost to cooling. This extra energy accelerates the outflow, increasing its velocity at the contact discontinuity between the wind and the interstellar medium to

$$v_e = \left(\frac{2\eta\sigma^2 c}{3f} \right)^{1/3} \simeq 925 \sigma_{200}^{2/3} f^{-1/3} \text{ km s}^{-1}, \quad (2)$$

where $\eta = 0.1$ is the radiative efficiency of accretion and $f \equiv f_g/f_c$ is a factor allowing for deviations of the gas-to-total density ratio f_g from the cosmological value (see King 2005, for derivation of v_e). An outer shock moves ahead of this discontinuity into the ISM, sweeping the latter up and compressing it. Adiabatic jump conditions give a velocity $v_{\text{out}} = 4/3 v_e$ for this forward shock (Zubovas & King 2012a). This heats the ISM to a temperature

$$T_{\text{sh}} = \frac{3}{16} \frac{\mu m_p v_{\text{out}}^2}{k} \simeq 2.2 \times 10^7 \sigma_{200}^{4/3} f^{-2/3} \text{ K}, \quad (3)$$

where k is Boltzmann’s constant and μm_p is the mean mass per particle. The particle density of the swept-up ISM is

$$n = \frac{2f_g \sigma^2}{\pi G \mu m_p R^2} \simeq 60 f \sigma_{200}^2 R_{\text{kpc}}^{-2} \text{ cm}^{-3}, \quad (4)$$

which is just 4 times the preshock particle density, as appropriate for a strong shock.

The interstellar gas which has passed through the outer shock is relatively dense, and so likely to cool quite rapidly below the shock temperature. The primary cooling process at the shock temperature is free-free cooling, and outflows are optically thin to this radiation:

$$\tau \simeq \kappa n \mu m_p R_{\text{sh}} \simeq 0.2 f \kappa \sigma_{200}^2 R_{\text{kpc}}^{-1}, \quad (5)$$

where we take $\mu = 0.63$, appropriate for fully ionized gas of Solar metallicity. The pressure within the shocked outflow is approximately constant (Zubovas et al. 2013a). Furthermore, the interface between the shocked wind and the outflow is highly Rayleigh–Taylor (RT) unstable (King 2010a, also see Section 3). RT fingers mix the shocked cooling interstellar gas with the dilute hot wind gas inside it, maintaining a constant pressure within the whole outflow. This pressure decreases over time as t^{-2} .

From the above considerations, the following picture of a composite outflow emerges. Most of the outflowing mass is in the form of the shocked ISM at temperatures below a few times 10^7 K. This gas is mixed (by RT instabilities) and maintains a pressure equilibrium with the much hotter shocked wind. We show this schematically in Figure 1. To determine the observational appearance of this mixture we need to consider whether the shocked ISM can be kept at these large temperatures for a long time.

3 OUTFLOW STABILITY

An important aspect of the thermal evolution of outflowing gas is its phase structure. The gas can either cool as a single-phase medium and experience strong compression by the shocked wind into a narrow shell, or it can develop a two-phase structure with cold gas embedded in the tenuous, high-pressure hot medium. Therefore we consider whether a multiphase equilibrium between cold gas clumps and a surrounding diffuse outflow is possible.

Following Krolik et al. (1981), we define a pressure-based ionization parameter

$$\Xi = \frac{L}{4\pi R^2 n k c T} = \frac{p_{\text{rad}}}{p_{\text{gas}}}, \quad (6)$$

where L is the quasar luminosity, which we take to be a fraction l of the Eddington luminosity, with the mass of the SMBH a fraction m of the critical M_σ mass (see Section 2), so that

$$L = \frac{4\pi G M c}{\kappa} l = \frac{4f_c \sigma^4 c}{G} m l. \quad (7)$$

Substituting the expressions for luminosity, density (eq. 4) and temperature (eq. 3) into eq. (6), we find

$$\Xi = 0.07 f^{-1/3} m l, \quad (8)$$

where we expect $l \simeq m \simeq 1$ in general.

Figures 4 and 5 of Krolik et al. (1981) show that for $\Xi \lesssim 0.5$ the outflowing gas can only be stable in a cold phase. The ionization parameter does not change as the outflow expands, because both radiation and gas pressures decrease as $p_{\text{rad}} \propto p_{\text{gas}} \propto R^{-2}$. Therefore, the only way to establish an equilibrium is to reduce the gas fraction f . As the gas cools and molecular clumps detach from the hot flow, the density in the latter decreases, but a reduction by a factor ~ 400 is necessary before equilibrium can be established. Therefore we predict that the diffuse gas envelope surrounding the molecular clumps is very tenuous, and almost all the outflow mass is in molecular form.

The separation of the outflow into a two-phase medium is not a new result. King (2010a) showed that energy-driven outflows are highly RT unstable, therefore a complicated mixture of shocked wind and outflow gas would emerge even without any cooling processes. Nayakshin & Zubovas (2012) used numerical simulations to show that cooling outflows fragment, but did not investigate the reasons for fragmentation in detail. Gravitational instability of expanding supernova shells was predicted analytically by Whitworth et al. (1994).

4 COOLING OF THE SHOCKED GAS

We now turn our attention to the efficiency of cooling processes acting in the shocked ISM. The outer shock temperature is approximately equal to the Compton temperature ($T_C \simeq 1.9 \times 10^7$ K), so Compton cooling – the primary process of cooling the shocked wind – does not affect the shocked ISM. Instead, at temperatures $T_g > 10^4$ K, gas predominantly cools via two-body processes, i.e. bremsstrahlung and metal line cooling. To estimate the cooling timescale, we numerically integrate the cooling function from Sazonov et al.

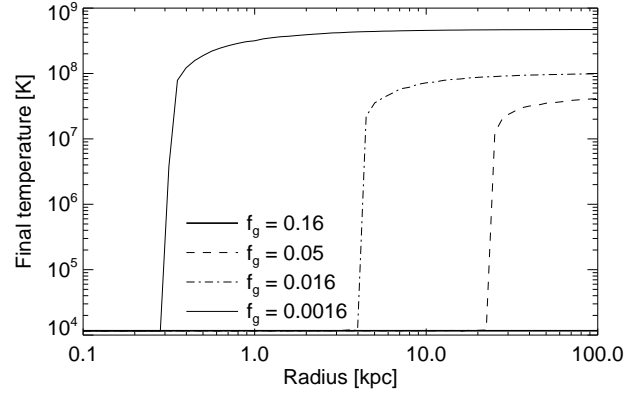


Figure 2. Temperature of shocked interstellar gas one dynamical time after the shock heats it, as a function of radius R . For low gas fractions and at large radii, radiative two-body cooling is inefficient, so the gas stays hot ($T > 10^7$ K). There is a sharp transition at a particular radius for every gas fraction; within this radius, gas is cool ($< 10^5$ K) and the resulting two-phase instability leads to the formation of molecules. The line at 1.1×10^4 K is a lower limit of our integrator rather than a physical barrier.

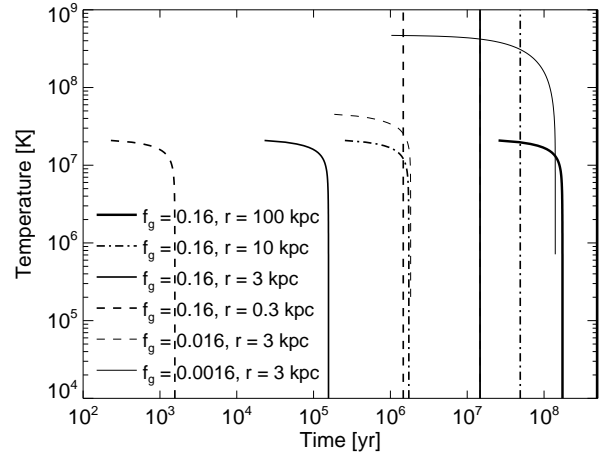


Figure 3. Cooling of pressure-confined gas in an outflow as function of time, for a range of gas fractions and outer shock radii. The gas is assumed to be stationary (assumption appropriate since cooling is faster than dynamical time). The cooling process is slow at first, but then accelerates rapidly as the gas begins to contract and Compton heating becomes inefficient. Vertical lines show dynamical timescales at certain radii (same line style as corresponding cooling curves of $f_g = 0.16$).

(2005, see their Appendix C for details), which is appropriate for optically thin gas illuminated by quasar radiation; as we showed above (eq. 5), this is a valid assumption. We perform the calculations for a range in gas fraction, f_g , between 1.6×10^{-3} and 1, and at distances from $R = 100$ pc to 100 kpc. For each of those, we integrate the cooling for one dynamical time $\sim R/\sigma$, assuming the pressure is constant and equal to that of the shocked wind gas.

The results are plotted in Figures 2 and 3. The first one shows the gas temperature after one dynamical time as a function of radius for several gas fractions f_g . There

is a clear difference between two regimes: low density gas far away from the SMBH cools inefficiently, while closer in or at higher density, cooling rapidly decreases gas temperature to the lower limit of the adopted cooling function, $T_{\text{low}} \simeq 1.1 \times 10^4$ K. A sharp transition seen in the low density curves ($f_g \leq 0.05$) can be identified as a cooling radius similar to the cooling radius (Zubovas & King 2012b) of the wind shock. From the integration results, we find this outer cooling radius to be

$$R_{\text{OC}} \simeq 100 f^{1.5} \text{ kpc}, \quad (9)$$

where ‘OC’ stands for ‘outflow cooling’. Therefore, as long as the gas density is $\gtrsim 0.05$ times the total density, the shocked interstellar gas in the central few kiloparsecs is efficiently cooled. As it cools, the gas is likely to fragment into cold clumps surrounded by a hot diffuse medium. A precise treatment of this fragmentation is beyond the scope of this Letter; we only note that Nayakshin & Zubovas (2012) showed the existence of such fragmentation numerically.

4.1 Molecular cooling processes

Once the gas temperature falls below a few times 10^4 K, atomic and molecular hydrogen and metal cooling become important. Calculating the effect of these elements precisely is very complicated, as cooling rates strongly depend on gas opacity, chemical abundance and various other local parameters. Here we only make a rough estimate. We take the cooling rate of atomic gas just below 10^4 K to be

$$\Lambda_{\text{mol}} \simeq 10^{-25} n'^2 \text{ erg cm}^3 \text{ s}^{-1}, \quad (10)$$

as given in Spitzer (1978, Chapter 6.2). This is a conservative estimate, as it does not include the contributions of metal lines or molecular hydrogen. The gas density appropriate for this cooling process is $n' \sim n T_{\text{sh}}/T_{\text{low}} \simeq 10^3 n$, because the clumps of atomic gas are much denser than the average density in the shocked ISM. Substituting eq. (4) gives the cooling rate

$$\Lambda_{\text{mol}} = 3.6 \times 10^{-16} R_{\text{kpc}}^{-4} f^2 \left(\frac{T_{\text{sh}}/T_{\text{low}}}{10^3} \right)^2 \sigma_{200}^4 \text{ erg s}^{-1}. \quad (11)$$

The corresponding cooling time, assuming the rate is constant, is

$$t_{\text{cool,mol}} \simeq \frac{3n' k T_{\text{low}}}{\Lambda} \simeq 24 \left(\frac{T}{1.1 \times 10^4 \text{ K}} \right)^2 R_{\text{kpc}}^2 f^{-1/3} \sigma_{200}^{-10/3} \text{ yr}. \quad (12)$$

This cooling timescale is much shorter than dynamical time for any reasonable value of R . We conclude that once gas cools down to atomic temperatures by two-body processes, the subsequent atomic and molecular cooling is very efficient, and rapidly puts most of the outflowing matter into molecular form.

5 STAR FORMATION IN THE OUTFLOW

Cold clumps of molecular gas, possibly shielded from the quasar radiation by envelopes of atomic hydrogen (the warm phase of the ISM), are perfect locations for star formation. As a result, we expect large-scale AGN outflows to form stars moving with large radial velocities. Such an effect was found

in numerical simulations by Nayakshin & Zubovas (2012) and Zubovas et al. (2013b), but they used only rough approximations for the rate of outflow fragmentation. Here we provide four estimates for an upper limit of star formation rate in the AGN outflow:

a) The cooling timescale estimate. This simply gives the rate at which gas in the outflow is converted into the cold molecular phase. The cooling timescale can be approximated by a power-law

$$t_{\text{cool}} \simeq 0.017 R_{\text{kpc}}^2 f^{-1.75} \text{ Myr}. \quad (13)$$

The total mass of the outflowing gas is

$$M_{\text{out}} \simeq 3 \times 10^9 R_{\text{kpc}} f \sigma_{200}^2 M_{\odot}. \quad (14)$$

Therefore, the approximate gas cooling rate is

$$\dot{M}_{\text{cool}} \simeq 1.8 \times 10^5 R_{\text{kpc}}^{-1} f^{2.75} \sigma_{200}^2 M_{\odot} \text{ yr}^{-1}. \quad (15)$$

This estimate, however, assumes that there is enough hot gas consumed by the outflow to be cooled down. This is not the case in reality, since the cooling timescale is typically faster than the flow timescale.

b) The ‘‘locally dynamical’’ estimate. Independently of how rapidly the gas cools, it cannot fragment faster than on its local dynamical timescale. For gas of density $n' = 10^3 n$, this timescale is

$$t_{\text{dyn}} \simeq 0.13 R_{\text{kpc}} f^{-1/2} \sigma_{200}^{-1} \text{ Myr}, \quad (16)$$

which translates into a star formation rate of

$$\dot{M}_{\text{dyn,local}} \simeq 2.4 \times 10^4 f^{3/2} \sigma_{200}^2 M_{\odot} \text{ yr}^{-1}. \quad (17)$$

c) The true parameter governing the rate of gas cooling and fragmentation is the rate at which the outflow sweeps up new mass:

$$\dot{M}_{\text{out}} \simeq 3750 f^{2/3} \sigma_{200}^{8/3} M_{\odot} \text{ yr}^{-1}. \quad (18)$$

These three limits scale differently with galaxy and outflow parameters, so the true dynamical limit is the lowest of the three. However, this is only the limit on gas cooling and fragmentation rate, because it does not account for star formation feedback.

d) A rough estimate of the true star formation rate can be made by assuming that star formation feedback (in the form of photoionization, massive star winds and supernova explosions) heats and disperses the cold gas. In this way, the star formation process self-regulates so that the feedback energy injected by the stars balances the cooling rate of the gas. The energy loss rate is

$$\dot{E}_{\text{cool}} \sim \frac{M_{\text{out}} k T_{\text{sh}}}{\mu m_{\text{p}} t_{\text{cool}}} \sim 3.2 \times 10^{46} R_{\text{kpc}}^{-1} f^{2.08} \sigma_{200}^{10/3} \text{ erg s}^{-1}. \quad (19)$$

The stellar feedback luminosity that affects the gas is

$$L_{\text{fb}} \sim \epsilon_{\text{f}} \epsilon_{\star} \dot{M}_{\star} c^2, \quad (20)$$

where $\epsilon_{\text{f}} < 1$ is a feedback coupling efficiency and $\epsilon_{\star} = 7 \times 10^{-3}$ is the stellar mass-to-luminosity conversion efficiency (Leitherer et al. 1992). Requiring that the feedback luminosity balances the cooling rate gives

$$\dot{M}_{\star} \simeq 80 \epsilon_{\text{f}}^{-1} R_{\text{kpc}}^{-1} f^{2.08} \sigma_{200}^{10/3} M_{\odot} \text{ yr}^{-1}. \quad (21)$$

Since not all of the stellar luminosity is absorbed by the surrounding material (due to both geometry and varying

opacity), the true upper limit to the star formation rate is somewhat higher.

The above estimate does not depend on the rate at which the outflow accumulates mass. If all the gas is cold, star formation still self-regulates at a value set by balancing the actual cooling of gas (heated by the stellar feedback processes rather than the forward shock) with the energy input rate.

This star formation rate results in a luminosity of young stars of $L_* \simeq \dot{E}_{\text{cool}}/\epsilon_f \simeq 8.3 \times 10^{12} \epsilon_f^{-1} R_{\text{kpc}}^{-1} f^{2.08} \sigma_{200}^{10/3} L_{\odot}$, comparable to or slightly higher than the luminosity of the AGN that drives the outflow.

5.1 Star formation efficiency

We make a rough estimate of the typical size of gravitationally bound fragments. Since the cooling timescale is much shorter than dynamical for most values of R and f , the outflowing gas cools and fragments in a very narrow region, defined by the cooling timescale t_{cool} and the sound speed in the post-shock gas $c_{\text{s,hot}} \simeq v_{\text{out}}$:

$$d_{\text{cool}} \sim v_{\text{out}} t_{\text{cool}} \simeq 21 R_{\text{kpc}}^2 f^{2.08} \sigma_{200}^{2/3} \text{ pc}. \quad (22)$$

If we assume that the clumps form from material initially distributed in regions with length scales of order d_{cool} , the clump mass is of order

$$M_{\text{clump}} \sim d_{\text{cool}}^3 \mu m_p n \sim 8600 R_{\text{kpc}}^4 f^{7.25} \sigma_{200}^4 M_{\odot}, \quad (23)$$

i.e. the clumps have masses typical of molecular clouds. The high outflow pressure ensures that their densities are much larger than typical for molecular clouds (Roman-Duval et al. 2010). For the same reason, their radii are also significantly smaller than d_{cool} .

Under normal conditions, the star formation efficiency per dynamical time in clouds of this mass is ~ 0.02 (McKee & Ostriker 2007). However, the star formation rate is probably somewhat higher here due to the high external pressure; in principle, the situation is the same as that of an AGN outflow compressing pre-existing dense structures in the galaxy, such as the galactic disc (Zubovas et al. 2013a). If we consider the estimate based on energy balance (eq. 21) as the true limit to the star formation rate, the efficiency then becomes

$$\epsilon_{\text{SF}} \simeq \frac{\dot{M}_*}{\dot{M}_{\text{out}}} \simeq 0.02 \epsilon_f^{-1} R_{\text{kpc}}^{-1} f^{1.42} \sigma_{200}^{2/3}, \quad (24)$$

which is > 0.02 since $\epsilon_f < 1$. On scales of individual clumps, the star formation efficiency might be significantly higher due to their large density (Kruijssen 2012). In this case, it would be larger cooling complexes that are affected and dispersed by self-regulating feedback.

6 DISCUSSION

The picture described here suggests that most of the gas in a spherically symmetric energy-driven AGN outflow is not thermally stable and cools to low temperatures as the outflow proceeds. Both two-body (bremsstrahlung and metal line) and atomic hydrogen cooling processes are very efficient and cool the gas to temperatures conducive to molecule formation. This happens on a timescale $t_{\text{cool}} \simeq 0.017 R_{\text{kpc}}^2 f^{-1.75}$

Myr, which is much lower than the dynamical timescale within a radius $R_{\text{OC}} \simeq 100 f^{1.5}$ kpc, where f is the ratio of gas density in the galaxy to the cosmic baryon density. This cool component is mixed in with much hotter tenuous gas from the shocked central wind, and partially entrained by it.

This picture compares favourably with observations of fast molecular outflows (Feruglio et al. 2010; Sturm et al. 2011; Rupke & Veilleux 2011). Zubovas & King (2012a) already showed that the predicted velocities ($\sim 1000 \text{ km s}^{-1}$) and mass outflow rates (several $1000 M_{\odot} \text{ yr}^{-1}$) are in broad agreement with expectations from the energy-driven phase triggered by the central SMBH mass reaching the critical $M - \sigma$ value (eq. 1). Our results here refine this picture: we show that most of the outflow appears in molecular form, despite its high velocity $v \sim 1000 \text{ km s}^{-1}$. Once again, this is consistent with observations of outflows (Cicone et al. 2012).

6.1 Dynamics of molecular clumps

The clumps of molecular gas have much higher densities than their surroundings and are less affected by the ram pressure of the AGN wind. As a result, they partially detach from the diffuse outflow and decelerate. Zubovas et al. (2013b) found the same result in numerical simulations of fragmenting outflows. In addition, Rayleigh-Taylor instabilities mean that even the diffuse shocked ISM does not expand uniformly, but instead has a spread of velocities below the formal outflow velocity calculated by Zubovas & King (2012a). This explains the fact that observed velocities of molecular outflows are typically lower than the formal $v_{\text{out}} = (4/3)v_e$ (see eq. 2).

6.2 Molecular gas distribution

As the outflow progresses, on average, regions closer to the black hole are denser and cooler than regions further away. This happens due to two reasons: the cooling rate decreases outwards, and the outer regions are shocked later, leaving them less time to cool down. Such a situation is consistent with observations of Cicone et al. (2012), which suggest that at least in the molecular outflow of Mrk 231, molecular gas has higher densities in the central regions than in the outskirts.

It is important to note that these calculations assume a spherically symmetric isothermal gas distribution in the galaxy. In a realistic galaxy, this assumption breaks down outside a few kpc from the centre. While this does not preclude the formation of molecular gas in the outflow, the cooling rate may be significantly reduced in the directions perpendicular to the galactic disc plane. In this case, the molecular outflow would appear more similar to a galactic fountain, with most clumps ejected close to the plane of the disc. The star formation rate in the outflow would be similarly reduced, and the existing star formation may be easily confused with star formation in the disc due to its location.

6.3 Structure and stability of the outflow

King (2010a) showed that in energy-driven outflows, the density contrast between the shocked wind and the shocked

ambient medium is of order 10^9 . This configuration leads to formation of strong RT instabilities in the contact discontinuity, which enhance mixing and maintain a constant pressure throughout the outflow (see Section 2).

Several authors found that RT instabilities may be suppressed under certain conditions. Mizuta et al. (2005) showed that recombination effectively suppresses the instability growth, at least on length scales $\sim 0.1 - 1$ pc. However, efficient recombination requires temperatures $< 10^5$ K and so is irrelevant for the gas immediately behind the shock. Instabilities with wavelengths shorter than the width of the cooling region, i.e. $\lambda \lesssim 20$ pc (see eq. 22) are not suppressed by recombination effects.

Another way of suppressing RT instabilities is by strong radiation pressure (Jiang et al. 2013). However, as we showed in Section 3, the ratio of radiation pressure to gas pressure is $\ll 1$ until almost all of the outflowing gas becomes molecular. Therefore, radiation pressure is also unable to stop RT instability from growing.

There may be other ways of stabilising the contact discontinuity, for example via magnetic fields (e.g., Jones & De Young 2005). But even in this case, short wavelength instabilities can grow (Vishniac 1983), leading to mixing across the discontinuity. Finally, once the shocked outflowing gas becomes gravitationally unstable, the resulting clumpiness allows some of the hot wind to leak out of the bubble, once again enhancing mixing.

The net effect of these instabilities is to maintain pressure equilibrium throughout the outflow. Even without the instabilities, the pressure varies only by a factor of a few from the contact discontinuity to the forward shock (Zubovas et al. 2013a), so the precise nature of the instabilities is not important to the overall picture of outflow cooling. Another important effect of RT fingers is that they produce a large number of shock fronts, which can accelerate particles to cosmic ray (CR) energies. Our model therefore predicts that CRs are produced in AGN unless all instabilities of the contact discontinuity are efficiently suppressed.

6.4 Survival of molecular clumps

Molecular clumps embedded in hot gas are subject to various processes that act to destroy them. Here we briefly review the effects of three processes: cloud evaporation, Rayleigh-Taylor instabilities and Kelvin-Helmholtz instabilities.

The timescale of cloud evaporation can be approximated using the expressions in Cowie & McKee (1977). Their equation (22), when rescaled appropriately, gives

$$t_{\text{evap}} \sim 4 \times 10^7 M_4 r_{\text{pc}}^{-1} T_7^{-5/2} \text{yr} \sim 6 \times 10^6 R_{\text{kpc}}^2 f^{6.83} \text{yr}, \quad (25)$$

where M_4 is clump mass in $10^4 M_\odot$ and r_{pc} its radius in parsecs. In the above expression, we used the clump mass estimate from eq. (23), the hot gas temperature from eq. (3) and estimated the radius from the assumption that the clump density is 10^3 times the particle density (eq. 4). It appears that in most situations, i.e. where $R_{\text{kpc}} > 1$ and $f \simeq 1$, large clumps survive for long enough to form a significant number of stars. However, the clumps should have a range of masses around the value given by eq. (23), and the smaller clumps can evaporate more rapidly. This echoes the numerical simulations of Marcolini et al. (2005), who find clouds with masses of order $200 M_\odot$ evaporating due to thermal

conduction over $t \sim 1$ Myr under similar conditions, although with the wind streaming past the clouds with large velocities.

Another aspect which increases the survival time of clumps in our model is their rapid radial motion. The evaporation timescale scales with the square of the distance, so as the clump moves outward, it is progressively less affected by evaporation.

Rayleigh-Taylor instabilities can in principle develop at the clump interface, since the clump is much denser than the wind. Several authors have found, however, that in hot environments, hydrogen recombination (Ricotti 2014) and thermal conduction (Marcolini et al. 2005) suppress the growth of these instabilities. Therefore we are confident the RT instabilities do not destroy the clumps rapidly enough to prevent them from being observed at large distances.

Finally, Kelvin-Helmholtz instabilities can develop and disrupt the clumps, but only if the shear velocity between the clump and the diffuse outflow gas is large. Within our model, clumps form from the fast-moving gas, and therefore move with roughly the same velocity, i.e. $v_{\text{rel}} = |v_{\text{out}} - v_{\text{cl}}| \ll v_{\text{out}}$, so the KH instability growth timescale $t_{\text{KH}} \sim \sigma/v_{\text{rel}} t_{\text{dyn}} \gg t_{\text{dyn}}$.

Our discussion here is brief, since a more detailed treatment of clump dynamics after formation is beyond the scope of the paper. Nevertheless, even if some process destroys the clump soon after formation, the clump gas only adds to the hot outflow. The hot gas then cools down and forms clumps again, and the system potentially ends up in a cycle of cooling, clump formation, clump destruction and heating, so that there is a large amount of molecular gas present in the outflow at any given time.

6.5 Outflow visibility

There are other signatures of AGN outflows in addition to molecular emission lines. The very high temperature of the wind shock close to the AGN should make these objects intrinsically luminous gamma-ray sources. Assuming that the bubble expands spherically with constant velocity v_e , we get the shocked wind temperature

$$T_{\text{bub}} = T_{\text{sh}} \frac{v_w^2}{v_{\text{out}}^2} \simeq 2 \times 10^{10} \text{K}. \quad (26)$$

At this temperature, a significant fraction of the thermal bremsstrahlung radiation is emitted as gamma-rays. The number density in the shocked wind gas, assumed constant throughout the bubble volume, is

$$n_{\text{bub}} = 0.01 \sigma_{200}^2 t_7^{-2} \frac{f_c}{f_g} \text{cm}^{-3}, \quad (27)$$

with $t_7 \equiv t/(10 \text{Myr})$ and assuming that the SMBH mass $M = M_\sigma$ (eq. 1). The total bremsstrahlung luminosity emitted in a bubble with volume $V = 4\pi v_e^3 t^3/3$ is

$$L_{\text{ff}} = 2.4 \times 10^{-27} V n_{\text{bub}}^2 T_{\text{bub}}^{1/2} \simeq 3 \times 10^{39} \sigma_{200}^6 t_7^{-1} \text{ergs}^{-1}, \quad (28)$$

This luminosity is small compared with the total kinetic power of the outflow $L_{\text{kin}} = 0.05 L_{\text{Edd}} \simeq 5 \times 10^{44} \text{erg/s}$. This suggests that gamma-ray emission might only be strong in the early phases of the energy-driven outflow. However, the strong shocks we predict also offer another route to producing them, as they can accelerate cosmic ray electrons and

produce gamma rays via inverse Compton or synchrotron emission. In both cases, strong molecular outflows are potentially rewarding targets for future gamma ray observatories. The cooling shocked outflow produces thermal X-rays. Both gamma rays and X-rays are observed in our Galaxy, where two gamma-ray bubbles disposed symmetrically on either side of the Galactic plane, surrounded by soft X-ray emission on the edges, were discovered using the *Fermi* satellite (Su et al. 2010). These features may be a local (but intrinsically much weaker due to low gas fraction) example of AGN feedback (Zubovas et al. 2011).

We also find that the expected self-regulating star formation rate in an outflow is large, reaching $\sim 100 M_{\odot} \text{ yr}^{-1}$ or more. The luminosity of these young stars can outshine the AGN itself, leading to the galaxy being classed as a LIRG or ULIRG. This misclassification might be one of the reasons why similar large-scale outflows are attributed to driving by stellar feedback. Even if the feedback energy injected by the young stars is larger than the AGN contribution, the ultimate cause of the whole process is AGN wind.

Another reason for attributing outflow driving to starbursts is the fact that the outflows we have considered here can persist for $\sim 10^8$ yr after the central AGN has turned off (King et al. 2011). Therefore, outflows should be detected much more often than the AGN that inflated them in the first place. This opens the possibility that most, if not all, galaxy-wide outflows are ultimately triggered by AGN. This seems particularly likely in cases where the outflow has high velocities, $v_e \gtrsim 1000$ km/s, since starburst-driven winds are unlikely to be capable of reaching such velocities (Sharma & Nath 2013).

7 SUMMARY AND CONCLUSION

In this paper, we showed that spherically-symmetric energy-driven AGN outflows are thermally unstable and rapidly cool down to temperatures below 10^4 K, freezing out into dense molecular clumps. This scenario explains the fact that observed AGN outflows are mostly composed of molecular gas moving at high velocities. These findings, together with previous work analysing the structure of such outflows, give the following predictions for outflow visibility:

- The shocked wind bubble emits gamma rays. Unfortunately, the expected luminosity of the whole bubble ($L_{\gamma} \leq 10^{39}$ erg/s) is too low to be detectable with present instruments.
- The hot diffuse outflowing gas creates a soft X-ray envelope around the gamma-ray bubble. Parts of this envelope may be visible close to galactic discs, where the ISM density is much larger than elsewhere in the bulge and halo.
- The cold clumps, which account for most of the outflow mass, are observable in molecular lines. They are unlikely to form in galaxies with depleted diffuse gas content, such as the Milky Way, but should be common in dense systems.
- Star formation in the molecular clumps proceeds at a rate of order $100 M_{\odot} \text{ yr}^{-1}$, enough for its luminosity to exceed the total luminosity of the AGN.
- Many outflows attributed to star formation may instead be energy-driven by AGN. A direct signature of this would be a central gamma-ray emitting bubble surrounded by an

X-ray emitting shell. Since the outflow must be energy-driven this in turn would imply a central black hole mass very close to the $M - \sigma$ value. Such AGN-driven outflows should be both faster ($v_e \gtrsim 1000 \text{ km s}^{-1}$) and more concentrated to the galaxy centre than those driven by starbursts.

ACKNOWLEDGMENTS

We thank Roberto Maiolino and Sergei Nayakshin for helpful discussions, suggestions and comments on the manuscript. We thank the referee, Biman Nath, for a very helpful report. KZ thanks the UK STFC for support in the form successively of a postgraduate studentship and a postdoctoral research associate position, both at the University of Leicester. KZ is funded by the Research Council of Lithuania grant no. MIP-062/2013.

REFERENCES

- Cicone, C., Feruglio, C., Maiolino, R., Fiore, F., Piconcelli, E., Menci, N., Aussel, H., & Sturm, E. 2012, *A&A*, 543, A99
- Cowie, L. L., & McKee, C. F. 1977, *ApJ*, 211, 135
- Faucher-Giguère, C.-A., & Quataert, E. 2012, *MNRAS*, 425, 605
- Feruglio, C., Maiolino, R., Piconcelli, E., Menci, N., Aussel, H., Lamastra, A., & Fiore, F. 2010, *A&A*, 518, L155+
- Jiang, Y.-F., Davis, S. W., & Stone, J. M. 2013, *ApJ*, 763, 102
- Jones, T. W., & De Young, D. S. 2005, *ApJ*, 624, 586
- King, A. 2003, *ApJL*, 596, L27
- . 2005, *ApJL*, 635, L121
- King, A. R. 2010a, *MNRAS*, 408, L95
- . 2010b, *MNRAS*, 402, 1516
- King, A. R., Zubovas, K., & Power, C. 2011, *MNRAS*, L263+
- Krolik, J. H., McKee, C. F., & Tarter, C. B. 1981, *ApJ*, 249, 422
- Krujissen, J. M. D. 2012, *MNRAS*, 426, 3008
- Leitherer, C., Robert, C., & Drissen, L. 1992, *ApJ*, 401, 596
- Marcolini, A., Strickland, D. K., D’Ercole, A., Heckman, T. M., & Hoopes, C. G. 2005, *MNRAS*, 362, 626
- McKee, C. F., & Ostriker, E. C. 2007, *ARA&A*, 45, 565
- Mizuta, A., Kane, J. O., Pound, M. W., Remington, B. A., Ryutov, D. D., & Takabe, H. 2005, *ApJ*, 621, 803
- Nayakshin, S., & Power, C. 2010, *MNRAS*, 402, 789
- Nayakshin, S., & Zubovas, K. 2012, *MNRAS*, 427, 372
- Pounds, K. A., King, A. R., Page, K. L., & O’Brien, P. T. 2003a, *MNRAS*, 346, 1025
- Pounds, K. A., Reeves, J. N., King, A. R., Page, K. L., O’Brien, P. T., & Turner, M. J. L. 2003b, *MNRAS*, 345, 705
- Pounds, K. A., & Vaughan, S. 2011, *MNRAS*, 415, 2379
- Ricotti, M. 2014, *MNRAS*, 437, 371
- Roman-Duval, J., Jackson, J. M., Heyer, M., Rathborne, J., & Simon, R. 2010, *ApJ*, 723, 492
- Rupke, D. S. N., & Veilleux, S. 2011, *ApJL*, 729, L27+
- Sazonov, S. Y., Ostriker, J. P., Ciotti, L., & Sunyaev, R. A. 2005, *MNRAS*, 358, 168

- Sharma, M., & Nath, B. B. 2013, ApJ, 763, 17
- Spitzer, L. 1978, Physical processes in the interstellar medium
- Sturm, E., et al. 2011, ApJL, 733, L16+
- Su, M., Slatyer, T. R., & Finkbeiner, D. P. 2010, ApJ, 724, 1044
- Vishniac, E. T. 1983, ApJ, 274, 152
- Whitworth, A. P., Bhattal, A. S., Chapman, S. J., Disney, M. J., & Turner, J. A. 1994, A&A, 290, 421
- Zubovas, K., & King, A. 2012a, ApJL, 745, L34
- Zubovas, K., & King, A. R. 2012b, MNRAS, 426, 2751
- Zubovas, K., King, A. R., & Nayakshin, S. 2011, MNRAS, 415, L21
- Zubovas, K., & Nayakshin, S. 2012, MNRAS, 424, 666
- Zubovas, K., Nayakshin, S., King, A., & Wilkinson, M. 2013a, MNRAS, 433, 3079
- Zubovas, K., Nayakshin, S., Sazonov, S., & Sunyaev, R. 2013b, MNRAS, 431, 793